NH_3 Adsorption on the Brönsted and Lewis Acid Sites of V_2O_5(010): A Periodic Density Functional Study

Xilin Yin, Huanmei Han, Isao Gunji, Akira Endou, S. Salai Cheettu Ammal, Momoji Kubo, and Akira Miyamoto*

Department of Materials Chemistry, Graduate School of Engineering, Tohoku University, Aoba-yama 07, Aoba-ku, Sendai 980-8579, Japan

Received: February 1, 1999

This paper deals with the adsorption states of ammonia on both the Brönsted and Lewis acid sites of V_2O_5-(010) surface using the periodic boundary first-principles density functional (DFT) calculations. The calculated results indicate that ammonia adsorption takes place on both the Brönsted and Lewis sites of V_2O_5 surface, whereas the adsorption on the Brönsted sites is found to be more favorable energetically. It is observed that ammonia adsorbs on the Lewis sites with different coverages, whereas stability under high coverage is low due to the steric repulsion derived from the coadsorbed ammonia molecules. In both the cases, it shows that the coordination interaction and hydrogen bonding between the N−H and vanadyl oxygen contributes to the binding energy. As for the adsorption on the Brönsted sites, it is found that the H-bonding plays a crucial role and that the ammonium species was formed when NH_3 adsorbs at the hydroxyl group containing the vanadyl oxygen. This is in agreement with the IR observations. Furthermore, it is confirmed that the hydroxyl group consisting of the vanadyl oxygen acts as the most reactive site for ammonia adsorption.

1. Introduction

Many different types of reaction mechanisms have been proposed for the selective catalytic reduction (SCR) of NO by NH_3 over V_2O_5 catalyst in the presence of oxygen.[1−26] The focus of the argument toward the SCR mechanisms is mainly the adsorption states of both NO and NH_3 molecules, which are directly related to the pathway of the reaction. In general, it is accepted that ammonia strongly adsorbs on the Brönsted site of V_2O_5 to form the NH_4^+ ion, which is followed by the SCR process.[2−17] However, different processes where the ammonia molecule is adsorbed on Lewis acid sites of the exposed vanadiums have also been reported.[18,19] Therefore, it is necessary to rationalize the adsorption states of ammonia on V_2O_5 in order to understand the mechanism. In addition, there are three kinds of Brönsted sites on the V_2O_5 surface[27] as a result of the existence of three kinds of structurally different lattice oxygens in layered V_2O_5: singly coordinated O_1, which is the vanadyl oxygen (V═O species), and dicoordinated O_2 and tricoordinated O_3, which bridge two and three vanadium atoms, respectively.

On the other hand, as a Lewis base, ammonia has also been used on metal oxides as a probe molecule to test the acidic properties of the surfaces experimentally,[28] as both Lewis and Brönsted acid sites exist on V_2O_5. The adsorption of ammonia on V_2O_5 reveals both Lewis and Brönsted acidity of the surface. It is well-known that surface acidity is an important property that often determines the surface chemistry and catalytic properties. The most commonly used method involves spectroscopic investigation of adsorbed probe molecules, and ammonia is one of the most common probe molecules. Ammonia is bonded to the surface mainly in two different modes. (1) The ammonia is protonated by a proton from a surface hydroxyl group. Therefore, it probes surface Brönsted acid sites. (2) The lone pair electron of the nitrogen atom is donated to the metal cation of the oxide, which acts as a Lewis acid.

However, a critical analysis of the bonding and mechanism behind both the SCR process and the acidity measured on the V_2O_5 surface is lacking, since little theoretical work accompanies the experimental measurements owing to the structural and chemical complexities of this oxide. Otamiri et al. have investigated the adsorption preferences of ammonia on the V_2O_5 non-hydroxyl surface in order to find out the critical step in ammoxidation processes by means of the extended Hückel/tight-binding calculations.[29] They pointed out that the on-top orientation of ammonia on the naked vanadium site is most stable, but a quantitative description in both energy and geometry with respect to the adsorption states is missing.

In addition, the activity of V_2O_5 lattice oxygens for the SCR reaction remains unresolved, and one of the key issues is that different active sites present in V_2O_5 have been proposed.[2−14] It is generally believed that the vanadyl oxygen plays the most important role in the SCR reaction and selective oxidation of hydrocarbons. Miyamoto and co-workers have investigated the SCR reaction catalyzed by the supported and unsupported V_2O_5 catalysts and pointed out that the O_1 oxygen acts as an active site.[2−6] Employing the cluster model, which consists of two V atoms and a hydroxyl group involving the vanadyl oxygen, Gilardoni et al.[13] have proposed that the vanadyl oxygen plays a key role in the SCR process, but they have not investigated the adsorption of ammonia on the other kinds of hydroxyl groups. In contrast to the generally accepted proposal with respect to the most important role of the O_1 atom in catalysis, Gasior et al.[14] have reported that the O_2 participates in the SCR reaction process.

In the present paper, we will focus on the binding states and energies of ammonia on both the Brönsted and Lewis acid sites present on the V_2O_5(010) surface to understand both the SCR reaction and the acidity measurement.

* Corresponding author. Phone: +81-22-217-7233. Fax: +81-22-217-7235. E-mail: miyamoto@aki.che.tohoku.ac.jp.

10.1021/jp990363p CCC: $18.00
Published on Web 05/15/1999

2. Methodology

2.1. Computational Details. The periodic density functional (DFT) calculations were performed by using the DSolid program,[30] within the Kohn−Sham formalism.[31] In this program the one-electron Schrödinger equations are solved only at the $k = 0$ wave vector point of the Brillouin zone. This program can be applied to systems that have small unit cells simply by ignoring this and treating them as having a larger cell, as described in the DSolid User Guide.[30] Geometry optimizations were carried out with the Vosko−Wilk−Nusair local-type functional (LDA),[32] whereas the interaction energies were computed using the B88-LYP (Becke 1988 exchange[33] with Lee−Yang−Parr correlation[34]) nonlocal-type functional (NLDA), which contains the necessary gradient corrections to eliminate the overestimations of the energy differences of the LDA. For weakly interacting systems, however, it is known that the B88 exchange functional underestimates the interaction energy or leads to potential energy curves without a minimum.[35,36] Molecular orbitals were expanded into a set of numerical atomic orbitals of doubly numerical + polarization (DNP) quality provided by the software package. The DNP is comparable in quality to Pople's split-valence 6-31G** basis set and usually yields the most reliable results.[37−39] To eliminate convergence problems in some cases, we allowed partial occupancies for the highest orbitals using smear values of less than 0.02 eV. To reduce the necessary CPU time, we froze the inner-core orbitals of the atoms except for hydrogen, whose pure potential was used; i.e., 1s was frozen for oxygen and nitrogen and 1s2s2p for vanadium. For the geometry optimization, the BFGS routine in which the gradients were computed numerically was employed.

2.2. Model. Experimental studies show that the V_2O_5(010) surface exhibits a key role in catalysis[40,41] and that the supported monolayer of the (010) surface has excellent catalytic activity.[42,43] Experimental[44] and theoretical[45−47] studies demonstrate that the (010) surface has physical properties and stability very similar to those of its bulk crystal. In the present work, the V_2O_5-(010) surface has been modeled by a periodic slab composed of a monolayer, where the optimized lattice parameters of a (11.535 Å) and c (3.603 Å) obtained from the CASTEP program were used.[45] The successive slabs along the b direction are separated by a vacuum region. The shortest distance between atoms belonging to successive slabs is greater than 20 Å, where the interlayer interaction is not significant. Therefore, it can be considered as a realistic model of the V_2O_5(010) surface.

Full optimization of all the constituent atoms of the adsorbate/substrate system was performed. The adsorption energy (E_{ads}) has been calculated according to the expression

$$E_{ads} = E_{(adsorbate/substrate)} - (E_{adsorbate} + E_{substrate})$$

where $E_{(adsorbate/substrate)}$, $E_{adsorbate}$, and $E_{substrate}$ are the total energies of the adsorbate/substrate system, isolated adsorbate, and substrate, respectively. A negative E_{ads} value corresponds to a stable adsorbate/substrate system.

3. Results and Discussion

Using the periodic boundary slab models, we have successfully described the geometric and electronic structures of V_2O_5-(010)[45] and investigated the adsorption properties of the hydrogen atom[27] and water molecule[48] on this surface. These studies have justified the reliability of both the surface model and approach that are employed in the present study.

TABLE 1: Bond Length (d_{N-H}) and Bond Angle ($\angle$H−N−H), Atomic Charge on Nitrogen (q_N) and Hydrogen (q_H) for Free Ammonia Molecule

geometry or charge	calcd	exptl[49]
d_{N-H} (Å)	1.023	1.012
$\angle$H−N−H (deg)	107.1	106.7
q_N	−0.577	
q_H	+0.192	

3.1. NH_3 Molecule. The equilibrium geometry and electronic structure of the free NH_3 molecule have been calculated using the periodic boundary cubic cell. The cell length is 8 Å, which can avoid the interactions among the equivalent cells. The fully optimized N−H bond lengths and H−N−H bond angles are shown in Table 1. It indicates that our calculated values are in good agreement with the experimental identifications,[49] again demonstrating the soundness of our methodology used in the current study.

Two kinds of dimer can be formed by an ammonia and a water molecule. A cubic cell with side $R = 10$ Å has been used to calculate the dimers. The calculated dimerization energy for the dimer with the hydrogen bond N−H····O is −1.2 kcal/mol (LDA value of −4.3 kcal/mol), and it is −6.9 kcal/mol (LDA value of −11.6 kcal/mol) for the dimer with the hydrogen bond O−H····N. The hydrogen bond lengths of the N−H····O and O−H····N are 2.118 and 1.933 Å, respectively. For the former dimer, the lone pair electrons of the oxygen were donated to the N−H antibonding orbital, and consequently, changes in the geometrical parameters of both molecules are observed. The amount of the net donated or accepted electrons is found to be 0.029 per molecule. Similar changes of the geometrical and electronic structures are observed for the latter dimer, and the net yield of donated or accepted electrons is calculated to be 0.048 per molecule.

3.2. On the Brönsted Acid Sites. It is generally believed that hydroxyl species present in metal oxide surfaces are formed mainly by the dissociation of water. Since our earlier study[48] shows that the H_2O molecule cannot dissociate on the stoichiometric V_2O_5(010) surface, in the present study, we use the hydroxyl V_2O_5 surface formed by atomic hydrogen adsorption on the three kinds of lattice oxygens[27] to mimic the real surface with various Brönsted acid sites.

At first, when the ammonia molecule approaches the three kinds of Brönsted acid sites on the V_2O_5(010) surface, it is observed that the NH_3 is strongly adsorbed on these sites (see Figure 1). As shown in Table 2, all three adsorption systems are calculated to be very stable energetically. It is also confirmed that the adsorption ability decreases in the order corresponding to the hydroxyl groups: O_1H > O_3H > O_2H. This order indicates that the adsorption of ammonia on the O_1H group is the most favorable, which is in good agreement with earlier observations.[2−13]

Furthermore, it is observed that one proton of the newly formed NH_4^+ ion at the O_1H site strongly interacts with the vanadyl oxygen adjacent to the O_1H species in the form of an H-bond with a distance of 1.58 Å, which is in agreement with the experimental identifications.[2−17] As a consequence, the corresponding N−H bond is elongated by 0.06 Å. Similarly, one proton of the NH_3 molecule adsorbed on the O_3−H species also interacts with the closest vanadyl oxygen through the H-bond by 1.86 Å. Although the proton of the O_3H also keeps a distance of 2.44 Å from its nearest O_2 site, at such a distance, the interaction is much less pronounced relative to the former H-bonding. Owing to the different strength of the interaction, the adsorption at the O_3H species is calculated to be weaker

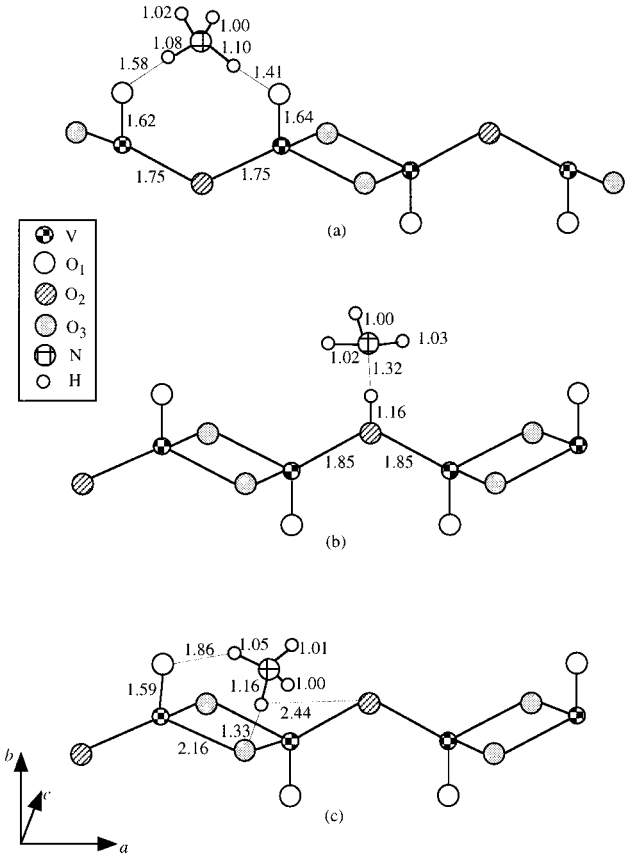

Figure 1. Geometries of ammonia adsorption at the Brönsted acid sites consisting of (a) singly coordinated oxygen, (b) dicoordinated oxygen, and (c) tricoordinated oxygen sites on V_2O_5(010). The values shown here designate the bond lengths (Å).

TABLE 2: Selected Parameters[a] of NH_3 Adsorption on the Brönsted Acid Sites of V_2O_5(010) Surface, the Corresponding Values before the Adsorption Given in Parentheses

adsorption sites	O_1H	O_2H	O_3H
q_N	−0.492 (−0.577)	−0.591 (−0.577)	−0.493 (−0.577)
q_H	+0.339 (+0.300)	+0.480 (+0.388)	+0.447 (+0.421)
q_O	−0.658 (−0.511) (−0.618)[b]	−0.688 (−0.567)	−0.764 (−0.621) (−0.678)[c]
q_V	+1.267 (+1.275) (+1.255)[b]	+1.163 (+1.180) +1.163 (+1.180)	+1.190 (+1.153) +1.190 (+1.153) +1.297 (+1.280)
$(NH_4)^{x+}$	+0.726	+0.712	+0.786
d_{N-H} (Å)	1.10	1.32	1.16
d_{O-H} (Å)	1.41 (0.97)	1.16 (0.98)	1.33 (0.99) (2.44)[d]
Δd_{O-H} (Å)	0.44	0.18	0.34
E_{ads} (kcal/mol)	−27.4 (−44.0)	−15.0 (−34.3)	−20.7 (−35.9)

[a] Charges (q) on the N, O, and V atoms as well as the H atom of the OH group, net charge on the adsorbed $(NH_4)^{x+}$ species, the newly formed bond distance (d_{N-H}), elongation of the O−H bond length (Δd_{O-H}), as well as adsorption energy (E_{ads}) (the LDA values are in parentheses). [b] Charges on the nearest atoms of the V═O group. [c] Charge on the nearest O_2 atom. [d] Distance between the H and the closest O_2 atom.

than that at the O_1H but still stronger than that of the O_2−H owing to the interaction of the NH_3 molecule at the O_2H species with its surrounding atoms. That is why the N−H bond length of the NH_3 molecule adsorbed at the O_2H species remains almost the same as that of the free NH_3 molecule.

On the other hand, it is found that the NH_3 molecule donates its electrons to the surface significantly (Table 2), and therefore, the surface becomes polarized. Such a redistribution of charges plays a very important role for adsorption systems, which has been confirmed by previous studies.[48,50−52] The ionicities of the three NH_4^+ ions are observed to be very different, and no correlation with their adsorption abilities is found. This phenomenon is very similar to that of the molecular adsorption of water on the clean V_2O_5(010) surface.[48] However, it is observed that the N atom of the NH_4^+ ion belonging to the most stable adsorption system (see Figure 1a) possesses the least negative charge, while the N atom of the least stable adsorption system (see Figure 1b) takes the most negative charge (Table 2). It seems that the charge on the N atom of the NH_4^+ ion is correlated with the corresponding adsorption ability. The same trend and correlation are observed for the H atom of the hydroxyl species.

When the charges on vanadiums connected to the interaction sites (Table 2) are compared, it is observed that these V atoms did not change their charges significantly. On the contrary, the O atoms belonging to the O_1H, O_2H, and O_3H groups increased their charges by 0.147, 0.121, and 0.143, respectively. This order is found to be the same as that of the corresponding adsorption ability.

As shown in Table 2, the length of the newly formed N−H bond in NH_4^+ ions decreases in the same order as that of the adsorption ability, which clearly shows that it is easier to release the proton of the O_1H species and subsequently to interact with the NH_3 molecule than the O_2H and O_3H species. Also, interatomic distances of the O−H species after the adsorption are significantly elongated, and the increase in the O−H bond length is found to correlate with the adsorption ability and length of the newly formed N−H bond.

According to the above discussion, the adsorption ability of NH_3 at the hydroxyl species seems to be determined by the ability to provide lone pair electrons of the hydroxyl oxygens to the adsorbed NH_3 species rather than the electron-transfer ability from the adsorbate to the surface. This nature is found to be very similar to that of the molecular adsorption of water on the surface oxygens of V_2O_5.[48]

3.3. On the Lewis Acid Sites. It is well-known that both V_2O_5 and MoO_3 have layered structures. Owing to the existence of the long V−O bond of ca. 2.82 Å, V_2O_5 exposes several naked vanadiums that are chemically active as Lewis acid sites on the surface. On MoO_3 surface, however, there exist only short Mo−O bonds, indicating that the MoO_3 surface shows somewhat reduced activity relative to the V_2O_5 catalysts. Probably this difference leads to the significant difference in adsorption states and catalytic properties.

Our previous study[45] shows that the "naked" surface V atoms seem to be more reactive than that of the bulk. Adsorption of NH_3 on the Lewis acid site depends on the interaction of its frontier orbitals with the vanadium atoms. The exposed V atoms are electron-deficient and can receive electrons from the nitrogen lone pair orbitals of NH_3 through interaction of symmetry-related vanadium and NH_3 orbitals. Owing to the difference in the nature of interaction, the adsorption on the Lewis acid sites can be expected to be much weaker than that on the Brönsted acid sites where stronger interaction takes place. Considering the B88 functional used in this study, which underestimates the interaction energies for a weak interacting system,[35,36] it is reasonable to get lower adsorption energies. The fully relaxed geometry (Figure 2) shows that ammonia adsorption takes place on the Lewis acid site by two forms: The electron pair of the ammonia molecule is donated to the vanadium site, which leads to the formation of the V−N bond almost perpendicular to the surface

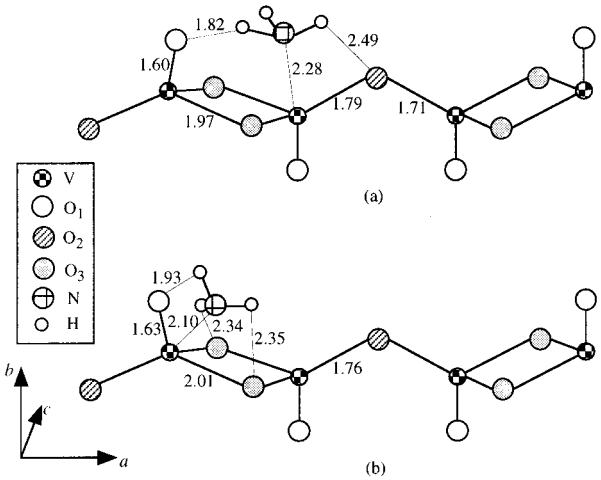

Figure 2. Fully optimized geometries of monoammonia molecule adsorption on the Lewis acid (a) on-top (T) and (b) bridging sites present in the V_2O_5(010) surface. The values shown here represent the bond lengths (Å).

TABLE 3: Optimized Interatomic Distances and Adsorption Energies (per NH_3 Molecule, the LDA Values Are in Parentheses) with Respect to NH_3 Adsorption on the Lewis Acid Sites of V_2O_5(010)

adsorption sites	T[a]	B[a]	B and T[a]	T and T[a]
d_{V-N}	2.28	2.10	2.06	2.44
			2.39	2.43
d_{O1-H}	1.82	1.93	1.82	1.89
			2.13	2.18
d_{O2-H}	2.47	2.96	3.01	2.78
			2.58	2.57
d_{O3-H}	2.60	2.34; 2.35	2.29	2.53
			2.39	2.62
E_{ads} (kcal/mol)	−2.3	−1.4	−1.0	+0.48
	(−30.6)	(−30.3)	(−23.3)	(−18.0)

[a] T represents the adsorption at the on-top site, and B denotes the adsorption at the bridging site. The details are in the text and Figures 2 and 3.

plane (on-top site, labeled T); the ammonia binds to both the singly coordinated oxygen and its counterpart vanadium (bridging site, B). The adsorption energies (Table 3) of both the above configurations are calculated to be very close and show that the former is slightly more stable than the latter by 0.9 kcal/mol. Owing to the weak interaction, as predicted, these energies are found to be much lower than the cases on the Brönsted acid sites.

The above results reveal that the coordination interaction between the N and V site plays a very important role in bonding. On the other side, it is found that the hydrogen bonding contributes rather significantly, since the H-bond lengths are observed to be 1.82 Å for T and 1.93 Å for B. The equilibrium interatomic distances of the two adsorption systems support the aforementioned similarity of their stability (Table 3). The bonding distances indicate that the interaction between the N and V site for T is weaker than that of B, but the H-bonding contributed mainly by $O_1\cdots H-N$ for the former is stronger than the latter. This suggests that the similarity in the interaction leads to a similar stability order.

As demonstrated in Table 4, the ammonia molecule donated 0.258 and 0.394 electrons to the substrate for the adsorption T and B, respectively, and as a consequence, the surface is observed to be polarized, which is similar to the case of the hydroxyl surface. The selected atomic charges regarding the adsorption on the Lewis sites are listed in Table 4. The Lewis

TABLE 4: Selected Charges on the N, H, V, and O_1 Atoms for NH_3 Adsorption on the Lewis Acid Sites of V_2O_5(010) Surface

adsorption sites	T[a]	B[a]	B and T[a]	T and T[a]	before adsorption
q_N	−0.567	−0.506	−0.536	−0.553	−0.577
			−0.556	−0.567	
q_H	+0.290	+0.286	+0.276	+0.282	+0.192
			+0.292	+0.296	
q_V	+1.142	+1.108	+1.129	+1.205	+1.272
			+1.190	+1.189	
q_{O1}	−0.515	−0.548	−0.571	−0.522	−0.324
			−0.453	−0.481	
$(NH_3)^{x+}$	+0.258	+0.394	+0.364	+0.164	0.000
			+0.197	+0.197	

[a] Notation as in Table 3.

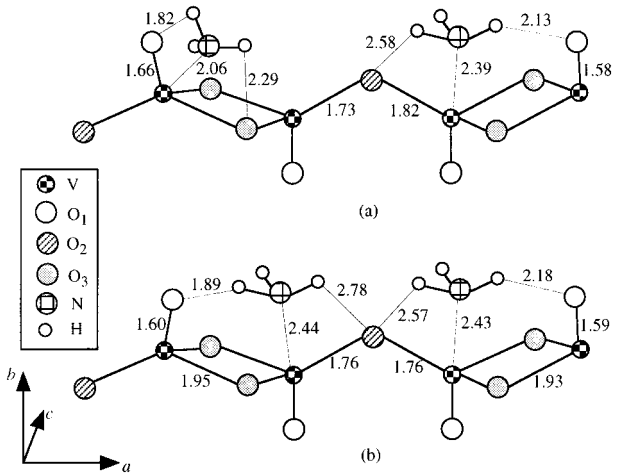

Figure 3. Equilibrium bond lengths (Å) of ammonia coadsorption on the Lewis acid sites of (a) B and T and (b) T and T on the V_2O_5(010) surface. Notation of B and T is as in Figure 2.

acid sites (V atoms) for the two systems are observed to be reduced. This reveals that the vanadiums accepted the lone pair electrons of the nitrogen belonging to the ammonia species. Indeed, charges on the corresponding N atoms decreased, which support the above speculation. In contrast, the O_1 atoms, which participate in H-bonding, are found to accumulate charge very significantly, indicating that the nature of the H-bonding present in these systems is different from that of H-bond $O\cdots H-N$ formed by H_2O and NH_3. For the latter H-bond, it was observed that the lone pair electrons of the O atom were transferred to the H−N, and therefore, charge on the O was decreased.

There might be a donation of a lone pair of electrons from the O_1 site to the NH_3 molecule, as in the case of the H_2O and NH_3 dimer. The net result shows that this donation is rather weak, and it is dominated by the back-donation of the N−H bonding electrons from the NH_3 molecule to the O_1 site. It is observed that this donation from the surface oxygen to the NH_3 molecule is less compared to the back-donation, since this oxygen is connected to the transition metal atom (V) and has less negative charge. All these result in the weakening of both the N−H and V−O_1 bonds. The donation and back-donation are very similar to that of H_2O adsorption on the surface oxygens of V_2O_5.[48]

Next, coadsorption of NH_3 molecules on the surface is investigated. When an NH_3 molecule approaches the surface, which is already attached to another ammonia molecule, the approaching NH_3 molecule is forced to adsorb at secondary adsorption sites as shown in Figure 3. The calculated adsorption energies demonstrate that the adsorption of the NH_3 molecules

on the Lewis acid sites took place (see Table 3). When the adsorption energies are compared, it is found that the adsorption of a second NH_3 molecule is weaker than that of the first NH_3 because of the steric repulsion between the adjacent coadsorbed NH_3 molecules. The coadsorption on bridging and on-top sites (B and T) is calculated to be more stable than that on two on-top sites (T and T) because the distance between the adjacent coadsorbed NH_3 molecules for the former is found to be longer than the latter, and so the two coadsorbed NH_3 molecules in the former case bear less repulsion.

When going from the geometric structure to the electronic one, similar to the monomolecular adsorption, the vanadium sites are found to accept the electrons transferred from the N atoms of NH_3 and are reduced. At the same time, the O_1 sites bound to the H atoms by H-bonds accumulated electrons, and accordingly, the charge is increased. Moreover, the coadsorbed NH_3 molecules transferred the charge to the surface, whereas the transferred charges on each site are observed to be less than that on the corresponding sites of the noncoadsorption (see Table 4). This finding seems to correspond to the weaker stability of the coadsorption systems. On the other hand, the nature of the electron transfer is found to be very consistent with that of the noncoadsorption. This consistency indicates again that the donation from the O_1 sites to the coadsorbed NH_3 is rather weak and that the back-donation of the N−H bonding electrons from the NH_3 to the O_1 sites plays a dominant role in bonding.

The results concerning NH_3 adsorption on the Lewis acid sites of V_2O_5(010) are found to be very similar to the experimental observations with respect to NH_3 adsorption on the TiO_2 surface.[54] That is, strong adsorption occurs at low NH_3 coverage, and it is attributed to specific Lewis acid−base adducts formed between NH_3 and exposed vanadium. A weakening in the strength of NH_3 adsorption occurs at high coverage because of repulsive lateral interactions between adjacent coadsorbed NH_3 molecules.

When the calculated adsorption energies as shown in Tables 2 and 3 are compared, the interaction of NH_3 with the Brönsted acid sites is found to be much stronger than that with the Lewis sites, indicating that NH_3 adsorption on V_2O_5 takes place preferably on the Brönsted sites rather than on the Lewis sites. This finding will contribute significantly to the understanding of the SCR reaction mechanism and acidity measurement.

4. Conclusions

Adsorption states of NH_3 on the V_2O_5 surface is a matter of controversy for a long time, which determines the understanding with respect to catalytic mechanisms, especially to that of the SCR reaction. In the present study, we have performed the periodic boundary DFT calculations to study the adsorption states of NH_3 on both the Brönsted and Lewis acid sites present in V_2O_5(010) surface. The results reveal that NH_3 adsorption takes place on both sites and that the adsorption on the Brönsted sites is found to be more favorable energetically. This finding provides very important information for understanding the SCR reaction mechanism and acidity measurement.

It is observed that NH_3 adsorbs on the Lewis sites with different coverages and that the stability under high coverage is weaker than that under low coverage because of the steric repulsion derived from the coadsorbed NH_3 molecules. In both the cases, it shows that the coordination interaction and hydrogen bonding between the N−H and vanadyl oxygen contribute to the bonding. As for the adsorption on the Brönsted sites, it is found that the H-bonding plays a crucial role and that the ammonium species was formed when NH_3 adsorbs at the O_1H group, which is in agreement with the IR observations. Furthermore, the hydroxyl group containing the vanadyl oxygen exhibits more reactive toward ammonia adsorption. The present study shows that the periodic DFT calculations are reliable for investigating the adsorption states of transition metal oxide catalysts.

References and Notes

(1) Bosch, H.; Janssen, F. *Catal. Today* **1988**, *2*, 369.
(2) Inomata, M.; Miyamoto, A.; Murakami, Y. *Chem. Lett.* **1978**, 799.
(3) Inomata, M.; Miyamoto, A.; Murakami, Y. *J. Catal.* **1980**, *62*, 140.
(4) Miyamoto, A.; Yamazaki, Y.; Hattori, T.; Inomata, M.; Murakami, Y. *J. Catal.* **1982**, *74*, 144.
(5) Miyamoto, A.; Inomata, M.; Hattori, A.; Ui, T.; Murakami, Y. *J. Mol. Catal.* **1982**, *16*, 315.
(6) Miyamoto, A.; Kobayashi, K.; Inomata, M.; Murakami, Y. *J. Phys. Chem.* **1982**, *86*, 2945.
(7) Topsøe, N.-Y.; Salbiak, T.; Clausen, B. S.; Srnak, T. Z.; Dumesic, J. A. *J. Catal.* **1992**, *134*, 742.
(8) Dumesic, J. A.; Topsøe, N.-Y.; Topsøe, H.; Chen, Y.; Slabiak, T. *J. Catal.* **1996**, *163*, 409.
(9) Topsøe, N.-Y.; Topsøe, H.; Dumesic, J. A. *J. Catal.* **1995**, *151*, 226.
(10) Topsøe, N.-Y. *Science* **1994**, *265*, 1217.
(11) Topsøe, N. Y. *J. Catal.* **1991**, *128*, 499.
(12) Topsøe, N. Y.; Topsøe, H.; Dumesic, J. H. *J. Catal.* **1995**, *151*, 241.
(13) Gilardoni, F.; Weber, J.; Baiker, A. *Int. J. Quantum Chem.* **1997**, *61*, 683.
(14) Gasior, M.; Haber, J.; Machej, T.; Czeppe, T. *J. Mol. Catal.* **1988**, *43*, 359.
(15) Takagi, M.; Kawai, T.; Soma, M.; Onishi, T.; Tamaru, K. *J. Phys. Chem.* **1976**, *80*, 430.
(16) Takagi, M.; Kawai, T.; Soma, M.; Onishi, T.; Tamaru, K. *J. Catal.* **1977**, *50*, 441.
(17) Luck, F.; Roiron, J. *Catal. Today* **1989**, *4*, 205.
(18) Ramis, G.; Busca, G.; Lorenzelli, V.; Forzatti, P. *Appl. Catal.* **1990**, *64*, 259.
(19) Lietti, L.; Svachula, J.; Forzatti, P.; Busca, G.; Ramis, G.; Bregani, F. *Catal. Today* **1993**, *17*, 131.
(20) Schneider, H.; Tschudin, S.; Schneider, M.; Wokaun, A.; Baiker, A. *J. Catal.* **1994**, *147*, 5.
(21) Janssen, F. J. J. G.; van den Kerkhof, F. M. G.; Bosch, H.; Rose, J. R. H. *J. Phys. Chem.* **1987**, *91*, 5921.
(22) Janssen, F. J. J. G.; van den Kerkhof, F. M. G.; Bosch, H.; Rose, J. R. H. *J. Phys. Chem.* **1987**, *91*, 6633.
(23) Chen, J. P.; Yang, R. T. *Appl. Catal. A* **1992**, *80*, 135.
(24) Chen, J. P.; Yang, R. T. *J. Catal.* **1993**, *139*, 277.
(25) Odriozola, J. A.; Heinemann, H.; Somorjai, G. A.; de la Banda, J. F. G.; Pereira, P. *J. Catal.* **1989**, *119*, 71.
(26) Ozkan, U. S.; Cai, Y.; Kumthekar, M. W. *J. Catal.* **1994**, *149*, 375.
(27) Yin, X.; Han, H.; Endou, A.; Kubo, M.; Teraishi, K.; Chatterjee, A.; Miyamoto, A. *J. Phys. Chem. B* **1999**, *103*, 1263.
(28) Kung, H. H. *Transition Metal Oxides: Surface Chemistry and Catalysis*; Elsevier: Amsterdam, 1989.
(29) Otamiri, J.; Andersson, A.; Jansen, S. A. *Langmuir* **1990**, *6*, 365.
(30) *DSolid User Guide*; MSI: San Diego, 1996.
(31) Kohn, W.; Sham, L. J. *Phys. Rev. A* **1965**, *140*, 1133.
(32) Vosko, S. H.; Wilk, L.; Nusair, M. *Can. J. Phys.* **1980**, *58*, 1200.
(33) Becke, A. D. *J. Chem. Phys.* **1988**, *88*, 2547.
(34) Lee, C.; Yang, W.; Parr, R. G. *Phys. Rev. B* **1988**, *37*, 786.
(35) Wesolowski, T. A.; Ellinger, Y.; Weber, J. *J. Chem. Phys.* **1998**, *108*, 6078.
(36) Jursic, B. S. *J. Mol. Struct.: THEOCHEM* **1998**, *434*, 29.
(37) Frisch, M. J.; Pople, J. A.; Binkley, J. S. *J. Chem. Phys.* **1984**, *80*, 3265.
(38) Gordon, M. S.; Binkley, J. S.; Pople, J. A.; Pietro, W. J.; Hehre, W. J. *J. Am. Chem. Soc.* **1982**, *104*, 2797.
(39) Francl, M. M.; Pietro, W. J.; Hehre, W. J.; Binkley, J. S.; Gordon, M. S.; Defrees, D. J.; Pople, J. A. *J. Chem. Phys.* **1982**, *77*, 3654.
(40) Inomata, M.; Miyamoto, A.; Murakami, Y. *J. Phys. Chem.* **1981**, *85*, 2372.
(41) Inomata, M.; Mori, K.; Miyamoto, A.; Ui, T.; Murakami, Y. *J. Phys. Chem.* **1983**, *87*, 754.
(42) Saleh, R. Y.; Wachs, I. E.; Chan, S. S.; Chersich, C. C. *J. Catal.* **1986**, *98*, 102.
(43) Bond, G. C. *Appl. Ctatal. A* **1997**, *157*, 91.
(44) Poelman, H.; Vennik, J.; Dalmai, G. *J. Electron. Spectrosc. Relat. Phenom.* **1987**, *44*, 251.

(45) Yin, X.; Fahmi, A.; Endou, A.; Miura, R.; Gunji, I.; Yamauchi, R.; Kubo, M.; Chatterjee, A.; Miyamoto, A. *Appl. Surf. Sci.* **1998**, *130*−*132*, 539.

(46) Lambrecht, W.; Djafari-Rouhani, B.; Vennik, J. *J. Phys. C: Solid State Phys.* **1981**, *14*, 4775.

(47) Yin, X.; Endou, A.; Miura, R.; Fahmi, A.; Gunji, I.; Yamauchi, R.; Kubo, M.; Teraishi, K.; Miyamoto, A. *Comput. Mater. Sci.* **1999**, *14*, 114.

(48) Yin, X.; Fahmi, A.; Han, H.; Endou, A.; Ammal, S. S. C.; Kubo, M.; Teraishi, K.; Miyamoto, A. *J. Phys. Chem.*, in press.

(49) Lide, D. R., Ed. *Handbook of Chemistry and Physics*, 74th ed.; CRC Press: Boca Raton, FL, 1993 (reprinted from *Kagaku Benran*, 3rd ed.; 1984; Vol. II).

(50) Nalewajski, R. F.; Köster, A. M.; Bredow, T.; Jug, K. *J. Mol. Catal.* **1993**, *82*, 407.

(51) Nalewajski, R. F.; Korchowiec, J.; Tokarz, R.; Broclawik, E.; Witko, M. *J. Mol. Catal.* **1992**, *77*, 165.

(52) Nalewajski, R. F.; Korchowiec, J. *J. Mol. Catal.* **1991**, *68*, 123.

(53) Pittman, R. M.; Bell, A. T. *Catal. Lett.* **1994**, *24*, 1.